The version of record of this article, published in Computers, Environment and Urban Systems, is available online at the publisher's website: https://doi.org/10.1016/j.compenvurbsys.2026.102454.
Cite as: Wei, X., Biljecki, F., Liu, P., Lei, B., Van de Weghe, N., & Huang, H. (2026). Modeling adolescents' perception of cycling safety: A new approach using graph neural networks and street view imagery. Computers, Environment and Urban Systems, 128, 102454.

Modeling Adolescents' Perception of Cycling Safety: A New Approach Using Graph Neural Networks and Street View Imagery

Xiaobing Wei[a,b], Filip Biljecki[b,e,*], Pengyuan Liu[c,d], Binyu Lei[f], Nico Van de Weghe[a], Haosheng Huang[a,*]

[a]*Department of Geography, Ghent University, Ghent, 9000, Belgium*
[b]*Department of Architecture, National University of Singapore, Singapore, Singapore*
[c]*Urban Analytics Subject Group, Division of Urban Studies and Social Policy, University of Glasgow, Glasgow, United Kingdom*
[d]*Future Cities Lab Global, Singapore-ETH Centre, Singapore, Singapore*
[e]*Department of Real Estate, National University of Singapore, Singapore, Singapore*
[f]*School of Geography, Earth and Environmental Sciences, University of Birmingham, Dubai, United Arab Emirates*

Abstract

Perceived cycling safety remains a critical determinant of bicycle use among adolescents. Previous studies have highlighted the role of street environments in shaping safety perceptions, but most rely on spatial attributes (e.g., road infrastructure, land-use indices) and rarely incorporate the cyclists' visual perspective. This study proposes a multidimensional framework that integrates visual and spatial representations of urban streets to model perceived cycling safety. By embedding fine-grained visual indicators derived from street view imagery into the road network, this novel framework captures 31 features across six environmental dimensions. Existing studies typically model perceived cycling safety using only a road's own attributes, neglecting the influence of nearby roads. To address this limitation, we develop an improved Graph Convolutional Network that incorporates geographic context. It integrates layer-wise attention and an adaptive loss function to handle class imbalance and capture spatial dependencies. Explainable

*Corresponding authors: Haosheng Huang, Filip Biljecki
Email addresses: xiaobing.wei@ugent.be (Xiaobing Wei), filip@nus.edu.sg (Filip Biljecki), Pengyuan.Liu@glasgow.ac.uk (Pengyuan Liu), b.lei@bham.ac.uk (Binyu Lei), Nico.VandeWeghe@UGent.be (Nico Van de Weghe), haosheng.huang@ugent.be (Haosheng Huang)

artificial intelligence (XAI) techniques are applied to interpret feature importance within the spatial context, moving beyond linear assumptions of traditional models. The framework is applied to a perception survey focusing on adolescents in Ghent, Belgium. The proposed model achieves an overall accuracy of 83.1%, outperforming all baselines and presenting a major advancement in this domain. XAI analysis reveals that both texture complexity and color monotony of the built environment tend to reduce perceived cycling safety, while tree coverage has a positive effect. Overall, the framework offers an interpretable and scalable approach for mapping street-level safety perception, providing actionable insights for cycling-oriented urban design and the development of sustainable transport planning.

Keywords: Cycling safety perception, Human–environment interaction, Urban spatial context, Visual complexity, Model interpretability

1. Introduction

Cycling delivers substantial public health and environmental benefits, including reduced risks of obesity and diabetes, as well as lower traffic-related air pollution and greenhouse gas emissions (Wei et al., 2025; Biljecki and Ito, 2021). These benefits have led governments to actively promote cycling as a sustainable mode of urban transport. For example, the European Commission has adopted the 'Vision Zero' strategy, placing particular emphasis on increasing cycling uptake in urban areas (European Commission, 2019). Nevertheless, perceived cycling safety remains a critical barrier that deters cycling and limits uptake in many cities (Álvaro Fernández-Heredia et al., 2014; Manton et al., 2016; Ye et al., 2024; Olsson and Elldér, 2023; Martínez-Díaz and Arroyo, 2023).

This perceptual barrier varies across demographic groups, with adolescents representing a particularly important segment due to their high exposure to everyday cycling environments combined with limited traffic experience (Rahman et al., 2022; Basaran et al., 2021; Klos et al., 2023). Their vulnerability is further amplified by heightened sensitivity to environmental risk cues (Benoit et al., 2022; Rahman et al., 2022). In Belgium, almost 40% of cycling-related traffic accidents involve students commuting (Vias institute, 2023). In practice, adolescents' cycling experiences are embedded in routine, route-based mobility patterns, where safety perceptions are shaped through repeated exposure to spatially connected urban environments rather than single road segments. These early, cumulative safety experiences can substantially influence adolescents' cycling confidence,

travel habits, and ultimately their lifelong mobility choices, highlighting the importance of understanding perceived cycling safety within a broader spatial and contextual framework (Schönbach et al., 2020).

The inherent complexity of urban environments makes it challenging to identify the causal factors shaping travel experiences (Mertens et al., 2015). Existing research on perceived cycling safety has primarily examined individual characteristics such as age, gender, and socioeconomic status (Black and Street, 2014; Harvey et al., 2014; Bill et al., 2015), and has gradually expanded toward physical environmental factors (Manton et al., 2016; Benoit et al., 2022). Studies have shown that shaping urban spaces in line with users' experiences is essential for encouraging cycling (Olsson and Elldér, 2023), and that road attributes such as intersections, roadway width, and infrastructure quality influence perceived safety (Lawson et al., 2013; Aldred et al., 2018). Recently, human-centered approaches using street view imagery (SVI) have emerged to capture cyclists' eye-level visual experiences, further enriching the representation of street environments in cycling safety research (Ye et al., 2024; Zeng et al., 2024). Building on these developments, most SVI-based studies primarily rely on low-dimensional indicators, such as pixel-level proportions of streetscape elements (e.g., trees or buildings), which provide only a partial representation of cyclists' perceptual experiences. More broadly, perceived cycling safety arises from the interplay between visual attributes, spatial configurations of street space, and dynamic traffic contexts within the urban network. While prior work has contributed valuable insights into specific environmental components, the integrated modeling of these interacting dimensions remains limited.

Road segments, as the immediate geographical entities through which individuals interact with the urban environment, are commonly adopted as the spatial units for evaluating perceived cycling safety (Manton et al., 2016; Wu et al., 2018). Existing studies for modeling perceived cycling safety are mainly based on a road segment's own features, and ignore its geographic context (i.e., the influences of adjacent and nearby segments) (Cui et al., 2023; Ye et al., 2024). Moreover, conventional statistical and machine learning methods, though effective for variable-level analysis (Benoit et al., 2022; Lei et al., 2025), fail to account for the complex relationship and spatial structure within urban space.

To address this overarching gap, we develop a human-centered, multidimensional framework for modeling perceived cycling safety that explicitly integrates visual, spatial, and dynamic environmental factors within a network-based context. We leverage publicly available SVI and road network data to derive physical environment indicators reflecting human-centered interactions, including visual

complexity, spatial enclosure, and network characteristics. To capture geographic context and spatial dependencies, we propose an improved graph convolutional network (GCN) to model perceived cycling safety at the road-segment level. Furthermore, explainable artificial intelligence (XAI) techniques are employed to quantify the contributions of different environmental features.

To summarize, in this paper,

1. We propose a human-centered, multidimensional set of environmental features that includes landscape elements, traffic environment, network features, spatial configurations, and complexity to capture the interaction between urban settings and safety perception.
2. We develop a new GCN model integrated with XAI to predict and evaluate perceived cycling safety, capturing deep-level relationships between a target road segment and its 'geographic context', i.e., nearby segments. This approach accounts for spatial dependencies and class imbalance to model the complex link between physical features and perceived safety.
3. The framework is validated through a real-world case study in Ghent, Belgium, demonstrating its capacity to predict cycling safety and potentially offering actionable insights for urban planning.

2. Literature review

As a subjective yet behaviorally influential factor, perceived cycling safety has garnered growing attention due to its alignment with actual accident patterns and its potential to offer direct insights into how cyclists experience and evaluate the road environment (Winters et al., 2012; Haustein et al., 2020; Ye et al., 2024). This has led to a wide range of empirical studies that underscore the critical role of the physical environment in shaping safety perceptions. In terms of traffic, traffic volume and speed limits are considered to have significant impacts on perceived cycling safety (Aldred et al., 2018; Vandenbulcke et al., 2014). Infrastructure-related factors, including degree, road function, and street width, are also important contributors (Lawson et al., 2013; Manton et al., 2016). In addition, land use patterns are also believed to shape subjective safety perception (Cho et al., 2009). Most studies focus on using geographic quantitative methods to assess the effects of different environmental factors, while they often fail to capture cyclists' perceptual experiences of urban space, particularly the visual environment, which plays a crucial role in shaping safety perception (Schepers et al., 2014; Huber et al., 2024; Graystone et al., 2022).

In recent years, SVI has provided a new perspective for assessing cycling contexts, with advantages in representing fine-scale visual environments. Ito and Biljecki (2021) explored the use of SVI combined with computer vision (CV) and demonstrated its effectiveness in a more comprehensive assessment of cycling environments that are difficult to obtain from traditional datasets. With the increasing availability of SVI and the rapid development of CV methods, a growing body of research has begun to focus on detailed and complex characteristics of cycling environments. For example, previous studies have reported a positive association between street-level greenery and cycling activity. Gao and Fang (2025a) examined the relationship between visual features extracted from SVI and cycling volume, while Guo et al. (2026) adopted an end-to-end learning approach using SVI to verify the influence of visual environments on cycling trajectories. These studies highlight the strong potential of SVI to represent cycling environments, ranging from fine-grained environmental elements to holistic depictions of cyclists' visual surroundings.

Building on these advances, recent studies integrate computer vision based SVI features into models for predicting subjective cycling safety perception. Zeng et al. (2024) collected cycling environment evaluations from 50 volunteers across 500 SVI scenes and employed semantic segmentation to examine how visual environments influence perceived cycling safety. Similarly, Costa et al. (2024) and Ye et al. (2024) analyzed the nonlinear relationships between urban visual elements and perceived cycling safety based on semantic segmentation results of SVI. In addition, some studies have used SVI to explore how cycling environment characteristics affect cycling preferences. However, these studies primarily focus on the compositional aspects of visual elements, emphasizing the proportion of different elements within images. As a result, they have limited capacity to capture cyclists' real-world experiences and immersion within specific road spaces. The perceptual mechanisms involved in human-environment interaction remain insufficiently characterized in cycling safety perception research, which limits the ability of existing models to represent actual cycling experiences.

In reality, human environmental perception is a complex process that goes beyond landscape composition, involving spatial patterns of the urban settings and perceptual experiences (Kim, 1999; Wang et al., 2025; van Rijswijk et al., 2016; Kawshalya et al., 2022). Spatial patterns provide a cognitive foundation for individuals to interpret their surrounding environment (Garling et al., 1984). Cao et al. (2025) demonstrated that the spatial form of a scene significantly affects subjective perceptions of safety. These configurations shape the spatial relationship between individuals and their surrounding environment, thereby influencing

urban activity (Purciel et al., 2009). For instance, tall and narrow streets provide stronger visual shelter and can more easily enhance pedestrians' sense of safety (Harvey et al., 2015). Furthermore, perceptual experience is affected by the complexity of environmental information (Sanocki et al., 2015). Visual complexity, as a critical dimension, contributes to the cognitive load encountered in a given scene (Zhou et al., 2022; Porteous, 2013). In environmental psychology, cognitive load is closely associated with perceptions of safety (Tapiro et al., 2020). Recent research using SVI has quantified visual complexity to validate its significant relationship with perceived safety (Kawshalya et al., 2022). Elements such as texture, color, and landscape type are recognized as key components of visual complexity (Elsheshtawy, 1997; Heath et al., 2000; Arnold, 1993). Therefore, this study aims to develop a multidimensional feature framework from the perspective of cyclists to systematically examine how road environments shape perceived cycling safety.

From a methodological perspective, Geospatial Artificial Intelligence (GeoAI) provides an effective technical pathway for analyzing multidimensional interactions between urban spaces and human perception (Kang et al., 2023). GeoAI incorporates location and spatial relationships into artificial computational processes to enhance the discovery of spatial knowledge and understanding of human-environment relationships (Liu et al., 2023; Janowicz et al., 2020). In the existing literature, non-parametric statistical models and traditional machine learning methods are commonly used to assess the contribution of environmental indicators to perceived cycling safety (Manton et al., 2016; Ye et al., 2024). However, these approaches tend to simplify urban complexity and spatial interactions, making it difficult to reflect the systematic effects of urban environments. As a representative method of GeoAI, graph neural networks (GNNs) are particularly well-suited for modeling spatial topologies and have played a vital role in urban spatial modeling (Liu et al., 2023; Yap et al., 2023). Nippani et al. (2023) applied GNNs to predict road-level traffic accident rates, achieving a mean absolute error of less than 22%. Yu et al. (2020) employed graph convolutional networks (GCNs) combined with a generative adversarial framework to predict traffic conditions across road segments, demonstrating excellent performance. These findings demonstrate that GNNs effectively utilize spatial context information to capture the interaction mechanisms among spatial entities. To the best of our knowledge, this is the first study to apply GNNs specifically for modeling subjective cycling safety perception. Additionally, XAI models are valuable tools for interpreting the inner workings of AI models, offering quantitative insights into how input variables influence predictive outcomes (Chen et al., 2025a). Through the integration of GeoAI models, XAI supports our understanding of spatial processes and sheds

light on policymaking in practice (Liu et al., 2024; Lei et al., 2025). This study is motivated by addressing current deficiencies in spatial sensitivity and explanatory power in cycling perception studies. Therefore, it focuses on the integration of GNN and XAI techniques to identify and explain the spatial drivers of perceived cycling safety.

The literature review elucidates that SVI-based cycling environment assessment has grown rapidly in recent years, offering valuable support for capturing street-level visual environments. However, notable limitations remain in current models of perceived cycling safety. Existing studies tend to oversimplify perception by relying on compositional indicators, despite the inherently multidimensional and scenario-dependent nature of perceived safety. Also, insufficient integration of road network structures and spatial context prevents a systematic understanding of how cycling environments influence perception. Current models generally overlook the combined effects of spatial context and visual factors experienced during cycling, thereby limiting their explanatory power and practical applicability.

To address these limitations, this study aims to propose a multidimensional cycling environment representation that integrates SVI and CV techniques. An enhanced graph convolutional network is employed to explicitly incorporate spatial context and model the relational structure between road segments. In addition, XAI methods are applied to identify and interpret the key visual and spatial drivers of perceived cycling safety. Through this approach, the study seeks to advance the understanding of how perceived cycling safety is formed within complex urban environments.

3. Method

Our proposed multidimensional framework for modeling perceived cycling safety at the road-segment level consists of five steps (Figure 1):

1. Data collection (Section 3.1): Adolescent volunteers assessed the perceived safety of road segments along home-to-school routes using an online platform, which was categorized into three perception levels: unsafe, neutral, and safe.
2. Extraction of visual features from SVI (Sections 3.2.1 – 3.2.4): they were processed using image segmentation, depth estimation, and object detection to drive multidimensional indicators of landscape elements.

3. Network feature integration (Section 3.2.5): Structural features of the road network were computed, and the previously extracted visual indicators and safety ratings were matched onto the corresponding road segments.
4. GNN modeling and explanation (Section 3.3): We introduced a relational attention GCN (RAGCN) that integrates layer-wise attention and an adaptive loss function to model perceived safety levels of road segments. The model captures nonlinear relationships between environmental features and perceived safety, while also accounting for spatial dependencies through graph convolution that aggregates information from neighboring road segments. Model outputs were then interpreted using GraphLIME to identify the spatial contributions for each feature.
5. Application (Section 4.1): The framework was applied to the large-scale road network in Ghent, enabling the mapping of perceived cycling safety and its relationship with environmental attributes, and potentially providing evidence-based recommendations for street-level safety improvements.

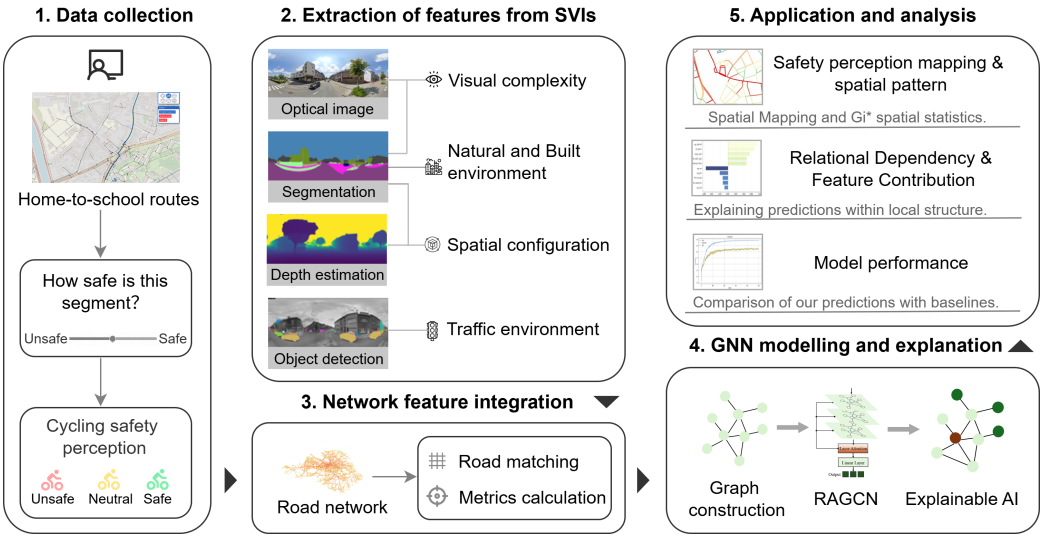

Figure 1: Our proposed framework for perceived cycling safety prediction.

3.1. Data and study area

Data collection. The survey was conducted from 1 September 2020 to 2 April 2021 through an online platform, the Bike Barometer, developed by Ghent Univer-

sity[1], aiming to capture how the city is experienced from a biking perspective. Participants were 12 to 18-year-old adolescents from the Flanders region in Belgium. As part of their GIS introduction lessons, they evaluated the perceived cycling safety of their home-to-school routes (Storme et al., 2022). In total, 2,353 participants took part in the survey across Flanders. Among them, over 600 participants were from the city of Ghent, which constitutes the focus area of this study and ensures a sufficiently large and representative local sample for subsequent analyses, consistent with prior findings on adequate sample sizes for perceptual surveys (Gu et al., 2025). The cycling safety assessment of the road network constituted a critical component of the project. As students are familiar with their daily home-to-school routes, they were asked to trace them on a digital map, which ensured that the evaluated network corresponded to their experience. For each student, each road segment along the traced route received an individual safety rating reflecting his or her perception. To ensure data completeness, providing a score for every selected segment was mandatory. For detailed information on the survey design, see Benoit et al. (2022). The study was approved by the Ethics Committee of Ghent University Hospital (B670201940648).

While extensive, this dataset has not yet been exploited to examine how visual environments relate to perceived cycling safety. The initial analysis by Benoit et al. (2022) focused on descriptive perception patterns and general environmental associations. In this study, we considerably extend the original work by embedding safety perceptions into the road network and integrating visual and spatial features within a multidimensional and explainable graph-based modeling framework, adding an entirely new dimension to this line of research.

Study area. Ghent was selected as the study area because of its high cycling modal share among students (approximately 30%), sustained investments in cycling infrastructure, and its strong policy focus on perceived cycling safety (Janssens et al., 2020; EU Urban Mobility Observatory, 2025). To ensure consistency with the survey coverage and enable detailed street-level environmental analysis, we delineated the study boundary using the spatial extent of all surveyed road segments in Ghent. We then expanded this extent to a polygon encompassing a 100-m buffered zone around the road network (Figure 2). This buffer captures adjacent environmental features that may influence perceived cycling safety. The final delineated area includes Ghent's primary urban district and part of its surrounding regions, representing diverse urban forms and cycling environments.

[1] `https://fietsbarometer.ugent.be`

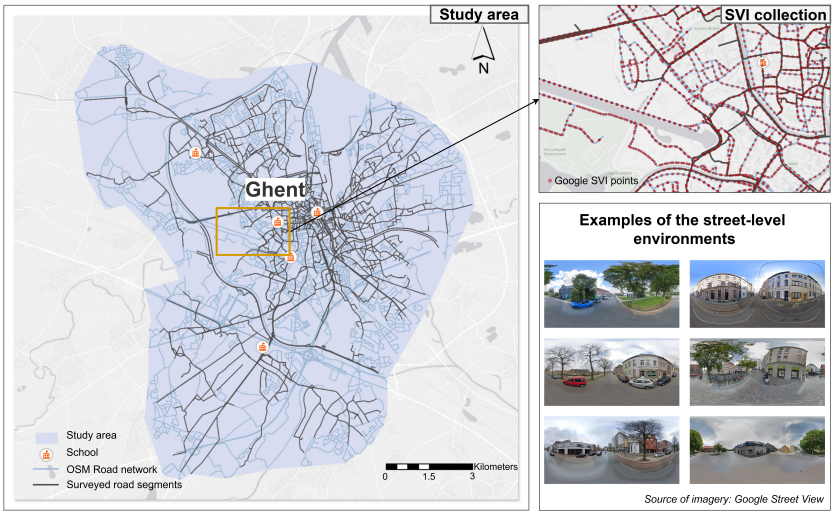

Figure 2: Map of the study areas and surveyed school locations.

Data processing and labeling. The road network data were obtained from OpenStreetMap (OSM), and processed using OSMnx to construct a topologically consistent road network graph. The surveyed road dataset was collected and linked to OSM roads to allow joint analysis of network attributes and street-level visual features. To accurately integrate adolescent-assessed safety ratings into the OSM road network, we adopted a systematic network matching procedure inspired by the iterative matching method proposed by Zhang and Meng (2007). Candidate matches were first identified within a 5 m spatial buffer and then refined based on geometric similarity and topological relationships, thereby ensuring precise and reliable segment alignment.

For data labeling, perceived cycling safety prediction was formulated as a three-class classification task, categorizing each road segment as unsafe, neutral, or safe, following prior research (Ye et al., 2024; Wu et al., 2018). During the survey, participants rated their perceived cycling safety on a 0-10 sliding scale, with 5 as the neutral midpoint. Accordingly, scores of 0-4 were labeled as unsafe, 5 as neutral, and 6-10 as safe. This discretization reduces ambiguity between raters with differing response tendencies, for example, between generous raters assigning 8-10 to safe roads and conservative raters assigning 6-8 for the same segments. For each road segment, the median value of all its ratings was adopted as the ground-truth label for model training and validation. Median aggregation is widely recognized as a robust method in studies involving human perception and rater behavior, providing a robust central tendency measure that mitigates the

influence of outliers (Garcin et al., 2013; Lakshminarayanan and Teh, 2013).

3.2. Environmental features for street space

In this study, a road segment is defined as the portion of a roadway between two adjacent intersections. To simulate the influence of real urban spaces on perceived cycling safety, each segment is regarded as a spatial unit that integrates visual environment and road characteristics, serving as a representation of the physical environment. For a given road segment s, the environmental feature vector is defined as $\mathbf{S}_F(s) = \{f_1, f_2, \ldots, f_{31}\}$, where f_i denotes the ith environmental feature. To provide a holistic characterization of the cycling environment, we developed a multidimensional environmental feature system encompassing six dimensions: built environment, natural environment, traffic environment, spatial configuration, visual complexity, and road attributes.

To implement this representation, we extracted these features using SVI and road network data, both of which are publicly available for many cities worldwide. SVI provide fine-grained information from the perspective of road users, particularly incorporating a vertical dimension, allowing a more realistic and comprehensive representation of the cycling environment (Biljecki and Ito, 2021). Leveraging computer vision techniques, we quantified environmental elements, traffic objects, and spatial depth to characterize the multidimensional street environment of each segment. SVI were collected from Google Maps[2] to capture the 360-degree view of the street. To ensure comprehensive coverage while avoiding redundancy, sampling points were generated at 50 m intervals along road segments, and at the midpoint for segments shorter than 50 m (Fan et al., 2025). In total, 30,060 panoramic SVI were collected within the study area. The acquisition time of the SVI mainly spans from 2020 to 2023. During this period, the built environment in the study area remained stable. The road network data contains the fundamental spatial units, whose geometric and functional attributes provide the physical basis for characterizing the street environment.

In the next five subsections (3.2.1–3.2.5), we describe the specific computational procedures used to derive indicators for each dimension of our environmental feature system, including: (i) visual natural and built environment features, (ii) traffic environment features, (iii) spatial configuration features, (iv) visual complexity features, and (v) road attributes.

[2] `https://www.google.com/maps`

3.2.1. Visual natural and built environment features

The composition of natural and built environment elements in a streetscape directly influences the initial perceptual phase of the urban scene (Dacey et al., 2005). To quantify these elements, we applied semantic segmentation to each image at the pixel level, where each pixel was assigned to the most probable streetscape category. Segmentation was performed using SegFormer, a state-of-the-art transformer-based model trained on the Cityscapes dataset. According to Xie et al. (2021), SegFormer reports a mean Intersection over Union (mIoU) of 81.3% on the Cityscapes benchmark dataset, demonstrating strong capability in delineating object boundaries. For each SVI, the proportion of pixels corresponding to a given environmental component was computed as its relative coverage within the streetscape. These values were then aggregated to the corresponding segment using the mean across all sampling points/SVI on the segment, as defined in Equation (1).

$$\bar{p}^{(t)} = \frac{1}{n} \sum_{i=1}^{n} p_i^{(t)} \tag{1}$$

Where, $\bar{p}^{(t)}$ represents the average proportion of pixels for environmental component t within a given segment, n is the number of SVI sampled along the segment, and $p_i^{(t)}$ denotes the proportion of pixels of component t in the i-th image.

To enhance interpretability and focus on features relevant to perceived cycling safety, only 9 Cityscapes classes that are common in urban streetscapes and potentially influential for safety perception were retained. The selected components were classified into two groups: natural environment features, including tree, grass, and sky; and built environment features, including building, wall, road, sidewalk, fence, and pole.

3.2.2. Traffic environment features

Urban traffic dynamics are critical to understanding perceived cycling safety, as interactions with motor vehicles and pedestrians significantly affect cyclists' risk perceptions (Chaurand and Delhomme, 2013; Kummeneje and Rundmo, 2020). Building on prior work demonstrating that street-level imagery can effectively capture urban mobility patterns (Zhang et al., 2019), we employed computer vision techniques to detect and quantify mobility-related objects within SVI. Although traffic features extracted from SVI represent snapshot observations, aggregating detections across multiple SVI along each segment offers a more stable approximation of local traffic activity, a practice commonly adopted in prior

SVI-based mobility studies (Zhang et al., 2019; Gao and Fang, 2025b). Object detection was performed using the Faster R-CNN model trained on the COCO dataset (Ren et al., 2016), selected for its proven robustness and high accuracy in streetscape element recognition. The analysis focused on traffic-related categories commonly examined in traffic safety studies (Yue, 2025), including cars, cyclists, pedestrians, motorcycles, buses, trucks, traffic lights, and stop signs.

For each road segment, the traffic environment was represented by the average count of each object category across all associated SVI, as defined in Equation (2):

$$\bar{o}^{(c)} = \frac{1}{n} \sum_{i=1}^{n} o_i^{(c)} \tag{2}$$

where $\bar{o}^{(c)}$ denotes the average count of traffic object c, n is the number of SVI associated with the road segment, and $o_i^{(c)}$ represents the count of object c in the i-th image.

3.2.3. Spatial configuration features

The three-dimensional configuration of urban settings plays an essential role in shaping human perception, influencing safety appraisal, comfort, and spatial awareness (Stamps III, 2005). *Enclosure* captures the degree to which vertical elements, such as building facades, trees, and roadside infrastructure, bound the observer's view (Ewing and Handy, 2009). *Visibility* refers to the longitudinal sight distance along a street corridor, capturing the perceived extent of clear and unobstructed view. Empirical research has confirmed that low visibility reduces the perceived safety of cyclists. (Friel et al., 2023). Together, these measures account for the vertical and horizontal dimensions of spatial configuration, representing key determinants of both psychological and functional qualities of urban space. Existing methods for quantifying these spatial attributes generally fall into two categories. The first employs 3D isovist models to calculate geometric metrics of visibility (Lonergan and Hedley, 2016), but struggles to incorporate fine-grained elements such as street trees or poles. The second directly measures the proportion of roads and surroundings from SVI (Rui and Xu, 2024), which captures human-scale perspectives but neglects the critical spatial metric of distance.

In our study, we proposed a depth-based approach that integrates monocular depth estimation with semantic segmentation to capture object-level distances from SVI (Figure 3). We employed the Metric 3D network (Yin et al., 2023), a self-supervised monocular depth estimation model achieving an absolute relative error of 0.0034 m on the KITTI benchmark (Geiger et al., 2012), to infer real-world distances from SVI pixels. Each 360° panoramic SVI was converted into

four monocular perspective views aligned with the cardinal directions (0°, 90°, 180°, 270°), representing forward, left, rear, and right views along the road, each with a horizontal field of view (FOV) of 90°. The transformation is defined as:

$$\mathbf{x}_{\text{view}} = R \cdot K^{-1} \cdot \mathbf{x}_{\text{pixel}}, \tag{3}$$

$$K = \begin{bmatrix} f & 0 & c_x \\ 0 & f & c_y \\ 0 & 0 & 1 \end{bmatrix} \tag{4}$$

where $\mathbf{x}_{\text{pixel}}$ is the pixel coordinate matrix, R is the rotation matrix for the target heading, and K is the intrinsic camera matrix. The focal length f is computed as:

$$f = \frac{0.5 \cdot W}{\tan(0.5 \cdot \text{FOV})} \tag{5}$$

where W is the output image width and (c_x, c_y) is the image center.

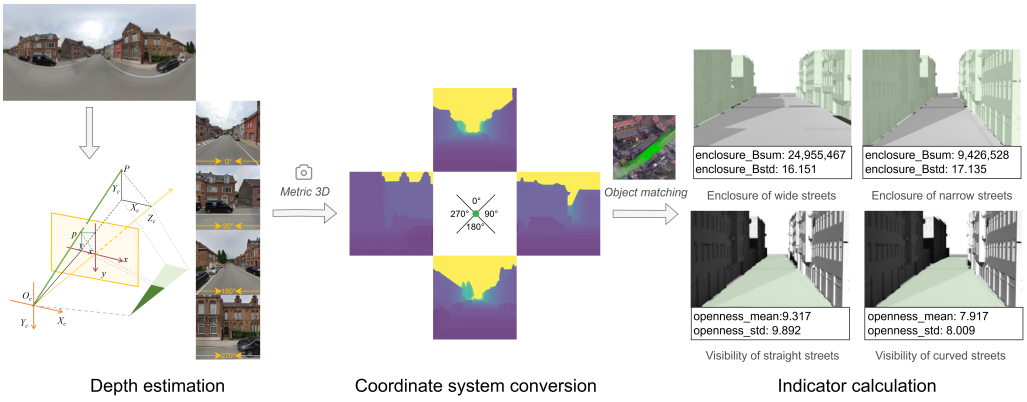

Figure 3: Depth-based approach for measuring spatial configuration metrics.

Depth estimation was applied to each directional view, producing depth maps where pixel values represent distances d_j^c (in meters) from the camera to visible surfaces, with a range of 0–80 m. These depth maps were then integrated with semantic segmentation results to obtain object-level depth distributions to quantify Enclosure and Visibility.

Enclosure is assessed separately for built environment elements (e.g., buildings, walls, fences, poles) and greenery elements (trees), focusing on features elevated

above ground level to reflect their contribution to perceived confinement. Following the 3D isovist framework (Kim et al., 2019), we computed for each category c two measures: the E^c, representing the cumulative visible distance (visual mass) of enclosing elements, and the V^c, capturing spatial heterogeneity of enclosure across the scene.

$$E^c = \sum_{j=1}^{N_c} d_j^c \tag{6}$$

$$V^c = \sqrt{\frac{1}{N_c} \sum_{j=1}^{N_c} \left(d_j^c - \bar{d}^c\right)^2} \tag{7}$$

Here, N_c is the number of pixels in category c, d_j^c is the depth of pixel j, and $\bar{d}^c$ is the mean depth. In this research, we have two categories: built environment or greenery.

Visibility is quantified as the longitudinal sight distance along the street axis, based on road surface pixels in the forward and rear views. We computed two measures: the O_{vis}, reflecting the average unobstructed distance along the corridor, and the D_{vis}, indicating variability in clearance that may reveal obstructions or geometric changes.

$$O_{vis} = \frac{1}{N_r} \sum_{j=1}^{N_r} d_j^{road} \tag{8}$$

$$D_{vis} = \sqrt{\frac{1}{N_r} \sum_{j=1}^{N_r} \left(d_j^{road} - \bar{d}^{road}\right)^2} \tag{9}$$

Here, N_r is the number of road pixels, d_j^{road} is the depth of pixel j, and $\bar{d}^{road}$ is the mean road depth.

3.2.4. Visual complexity features

The visual complexity features describe the overall visual impression of street environments, capturing the diversity and heterogeneity of elements that road users encounter. Visual complexity can influence perception, attention, and decision-making in transport settings, yet the micro-scale complexity of streetscapes is often underexplored (Guan et al., 2022; Kawshalya et al., 2022). In this study, complexity was evaluated across three perceptual aspects: color, texture, and object distribution.

Color complexity reflects the diversity of color distribution in the visual scene and constitutes an initial stage of human visual perception (Rietveld et al., 2020). To quantify this, we adopt the Herfindahl-Hirschman Index (HHI) (Chen et al., 2025b), which measures the degree of color concentration or dispersion. In our analysis, HHI was computed separately for the entire streetscape and the built environment mask:

$$C_t = \sum_{i=1}^{n} p_i^2 \tag{10}$$

where t denotes either the full image or the built environment mask, p_i is the proportion of pixels in the i-th color bin, and n is the total number of bins in the color histogram. Here, color distributions are derived from the joint histogram of hue (H) and saturation (S) in the HSV color space. The H–S combination provides a more sensitive and realistic characterization of color composition in street-level environment. Higher HHI values indicate dominance by a small number of colors, whereas lower values indicate greater color variability.

Texture complexity describes the structural arrangement and spatial variability of visual elements. We used the Gray-Level Co-occurrence Matrix (GLCM) entropy to capture texture irregularity by analyzing the spatial co-occurrence patterns of pixel intensities:

$$\mathrm{T}_t = -\sum_{i=1}^{n}\sum_{j=1}^{n} P(i,j)\,\log P(i,j) \tag{11}$$

where $P(i, j)$ denotes the joint probability of pixel pairs with gray levels i and j in the GLCM, and n is the number of gray levels (set to 64). Higher values indicate more complex and heterogeneous textures. Texture entropy is also computed for both the entire streetscape and the built environment mask. where $P(i, j)$ denotes the joint probability of pixel pairs with gray levels i and j in the GLCM, and n is the number of gray levels (set to 64). Higher values indicate more complex and heterogeneous textures. Texture entropy is also computed for both the entire streetscape and the built environment mask.

Object complexity represents the diversity of landscape element types present in the scene. We used an entropy metric (Cai et al., 2022), widely applied in land-use diversity analysis, to assess the distribution of object categories derived from the

segmentation results of SVI:

$$\mathrm{OE}_t = -\sum_{m=1}^{N} p_m \log p_m \tag{12}$$

where N is the number of object categories and p_m is the proportion of pixels belonging to category m within the image. Higher object entropy values indicate a greater diversity of elements in the streetscape.

3.2.5. Road attributes

In addition to micro-level streetscape features, we incorporated road attributes at the segment level. Three metrics are included: (1) degree, representing the number of directly connected segments; (2) segment length, defined as the geodesic distance between the start and end nodes of the road segment; and (3) road type, indicating the functional classification of the segment within the network.

Table 1 summarizes the 31 environmental variables across six dimensions and presents their descriptions.

Table 1: Summary of variables collected in this study.

Feature categories	Features	Meaning
Visual natural environment	`seg_tree`, `seg_grass`, `seg_sky`	Ratios of pixels segmented as trees/bushes, grass, and sky along the road segment.
Visual built environment	`seg_road`, `seg_sidewalk`, `seg_building`, `seg_wall`, `seg_fence`, `seg_pole`	Ratios of pixels segmented as built environment elements, including roads, sidewalks, buildings, walls, fences, and poles.

Continued on next page

Table 1 (continued)

Feature categories	Features	Meaning
Visual traffic environment	det_person, det_bicycle, det_car, det_motorcycle, det_bus, det_truck, det_traffic_light, det_stop_sign	Counts of detected traffic-related objects, including road users and traffic control elements, extracted from SVIs.
Visual complexity	texture_global, texture_builtenv	Texture entropy from the entire image and within the built environment mask.
	color_global, color_builtenv	Color complexity from the entire image and within the built environment mask.
	object_complexity	Entropy of landscape element types within the image.
Visual spatial configuration	enclosure_Tsum, enclosure_Tstd	Cumulative and variability measures of enclosure from trees/vertical vegetation.
	enclosure_Bsum, enclosure_Bstd	Cumulative and variability measures of enclosure from built structures (e.g., facades, walls).
	openness_mean, openness_std	Mean and variability of visibility distance from forward- and backward-facing SVIs.
Road attributes	degree	Number of adjacent segments (road connectivity).

Continued on next page

Table 1 (continued)

Feature categories	Features	Meaning
	`road_type`	Functional classification of the road segment, numerically encoded by hierarchy.
	`length`	Geodesic distance of the road segment.

3.3. Graph-based modeling and interpretation of perceived cycling safety

3.3.1. Residual and Attention-enhanced Graph Convolutional Network (RAGCN)

In urban road networks, road segments exhibit spatial dependence. As a result, perceived cycling safety of a road segment might be influenced by adjacent or nearby segments (Kwan, 2007). However, existing studies mainly model the perceived cycling safety of a road segment based on its own features, and ignore its "geographic context" (e.g., the influences of nearby segments) (Manton et al., 2016; Ye et al., 2024). We therefore propose a Residual and Attention-enhanced Graph Convolutional Network (RAGCN) to classify perceived cycling safety at the road segment level while accounting for these spatial dependencies. RAGCN builds on a classical three-layer GCN backbone and introduces residual skip connections, layer-wise attention, and normalization to capture multi-scale representations and improve training stability (Figure 4).

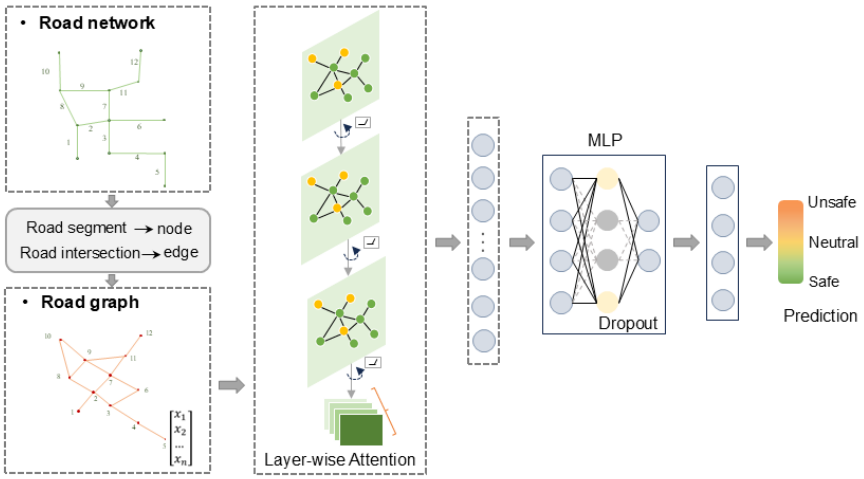

Figure 4: Architecture of the proposed RAGCN model.

We represent the road network as a spatial graph $G = (V, E)$, constructed from the road network data, where each node $v \in V$ corresponds to a road segment, and edges $e \in E$ represent topological connections between segments (Hamilton et al., 2017). The node feature matrix X encodes the 31 environmental variables previously defined, including visual features and road network attributes. The adjacency matrix $A \in \mathbb{R}^{n \times n}$ is constructed based on road segment connectivity, where n denotes the total number of road segments. The graph is treated as undirected. The focus of this study is on structural connectivity of the real environment.

The RAGCN model employs the standard GCN propagation rule:

$$Z^{(l)} = \sigma\left(\hat{A} Z^{(l-1)} W^{(l)}\right) \tag{13}$$

where $\hat{A} = \tilde{D}^{-1/2}(\tilde{A})\tilde{D}^{-1/2}$, $\tilde{A} = A + I$, and $\tilde{D}$ is the corresponding degree matrix. $W^{(l)}$ is the learnable weight matrix for layer l, $\sigma(\cdot)$ denotes the non-linear activation function (ReLU), and $H^{(l)}$ is the hidden representation at layer l.

To improve gradient flow and model stability, residual connections are introduced at each GCN layer, applied after activation and normalization to skip-connect the input of the previous layer with the current output:

$$\mathbf{H}^{(l)} = \sigma\left(\text{Norm}\left(\text{GCN}^{(l)}\left(\mathbf{H}^{(l-1)}\right)\right)\right) + \mathbf{H}^{(l-1)} \tag{14}$$

Here, $\text{GCN}^{(l)}(\cdot)$ denotes the graph convolution operation at the l^{th} layer, $\text{Norm}(\cdot)$ represents the normalization function, and $\sigma(\cdot)$ is the non-linear activation func-

tion (ReLU). The residual term $\mathbf{H}^{(l-1)}$ facilitates gradient flow during backpropagation, improving training stability in deeper networks.

Furthermore, a lightweight layer-wise attention mechanism is employed to adaptively weight the outputs of different GCN layers. Each layer representation $H^{(l)}$ is first projected by a learnable vector W_a to produce attention scores by a softmax function, which are normalized across layers:

$$\alpha^{(l)} = \frac{\exp\left(W_a H^{(l)}\right)}{\sum_{j=1}^{L} \exp(W_a H^{(j)})} \tag{15}$$

The final node representation is obtained as a weighted sum of all intermediate outputs, allowing the model to emphasize more informative depths:

$$H_{\text{final}} = \sum_{l=1}^{L} \alpha^{(l)} \cdot H^{(l)} \tag{16}$$

The model estimates the probability of each road segment being assigned to a class of perceived cycling safety (i.e., either "unsafe", "neutral", or "safe").

To address the issue of class imbalance in perceived safety labels, we employ a dynamically weighted hybrid loss function that combines Cross-Entropy (CE) Loss and Focal Loss (FL):

$$\mathcal{L}_{\text{total}} = \lambda_{\text{ce}} \cdot \mathcal{L}_{\text{CE}} + \lambda_{\text{fl}} \cdot \mathcal{L}_{\text{FL}}, \quad \lambda_{\text{ce}} + \lambda_{\text{fl}} = 1 \tag{17}$$

The adaptive weighting is realized by defining the coefficients as epoch-dependent:

$$\lambda_{\text{ce}}^{(e)} = \min\left(\lambda_0 + \frac{e}{E}(\lambda_{\max} - \lambda_0),\ \lambda_{\max}\right), \tag{18}$$

$$\lambda_{\text{fl}}^{(e)} = 1 - \lambda_{\text{ce}}^{(e)} \tag{19}$$

where e is the current epoch and E is the total number of epochs. This schedule gradually increases the CE weight while decreasing the FL weight, allowing the model to focus more on hard examples in the early stage and shift toward global stability in the later stage.

The two components of the hybrid loss are defined as:

$$\mathcal{L}_{\text{CE}} = -\sum_{i \in \mathcal{T}} \alpha_{y_i} \log p_{i,y_i}, \tag{20}$$

$$\mathcal{L}_{\text{FL}} = -\sum_{i \in \mathcal{T}} \alpha_{y_i} (1 - p_{i,y_i})^{\gamma} \log p_{i,y_i} \tag{21}$$

Here, α_{y_i} is the class-specific weight, γ is the focusing parameter, and p_{i,y_i} is the predicted probability of the true label.

3.3.2. Interpreting graph-based predictions

Bridging the model's internal representations with interpretable environmental factors is crucial for uncovering the mechanisms underlying perceived cycling safety and for translating analytical results into actionable urban insights. We employ GraphLIME (Huang et al., 2022), a local explanation method for GNNs,to interpret RAGCN predictions. The approach approximates the nonlinear decision boundary of the black-box model by fitting an interpretable linear surrogate model over the neighborhood of each target node. Formally:

$$\xi(v) \leftarrow \arg\min_{g \in G} \mathcal{L}(g, f, \mathbf{X}_n) \tag{22}$$

where $\xi(v)$ denotes the local explanation for node v, G is the space of interpretable models, f is the trained RAGCN, and $\mathbf{X}_n$ is the feature space of the neighborhood. This process yields node-level feature importance scores, revealing how environmental features influence safety perception across connected road segments.

3.3.3. Model implementation and evaluation

The proposed RAGCN model is implemented using PyTorch and Deep Graph Library (Wang et al., 2019). Training was conducted on Google Colab using the Adam optimizer with an initial learning rate of 0.005 for 500 epochs. A dropout rate of 0.1 was applied to prevent overfitting. Model performance was evaluated through Overall Accuracy (OA), Macro F1 Score, Weighted F1 Score, and Cohen's Kappa (Sokolova and Lapalme, 2009; Cohen, 1960), ensuring a balanced assessment of both global performance and sensitivity to minority classes.

4. Results

4.1. Preliminary analysis

After data cleaning (removing error records) and matching, we retained a total of 34,327 perceived safety ratings from 610 students in Ghent, covering 3,238 road segments with a combined length of approximately 876 km. Given that the total road network in the study area spans 2,773 km and consists of 11,477 segments, the evaluated segments represent 32.57% of the entire network, indicating substantial spatial coverage. The three perceived safety classes were distributed as follows: unsafe (20.2%), neutral (32.4%), and safe (47.4%). The distribution of the number of ratings per road segment and the within-segment variability (measured by IQR) are provided in Appendix B.

Figure 5 illustrates the correlation analysis between perceived cycling safety level and the environmental variables using Spearman correlation, without controlling for other factors. $Enclosure\_B_{sum}$ has a strong negative correlation with perceived safety, while $Enclosure\_T_{sum}$ has a strong positive correlation, suggesting that a greater spatial extent of visible trees is associated with higher perceived cycling safety among adolescents. In the traffic environment, the presence of pedestrians, buses, and cars is negatively associated with perceived safety, consistent with previous studies on traffic exposure and risk perception (Olsson and Elldér, 2023; Ferreira et al., 2022). Natural environmental features show positive correlations, suggesting that greener and more open environments are associated with higher perceived cycling safety. Road attributes, including road type, degree and length, also exhibit significant associations with safety perception. Built environment elements, including buildings, road surfaces, and poles, tend to have negative correlations.

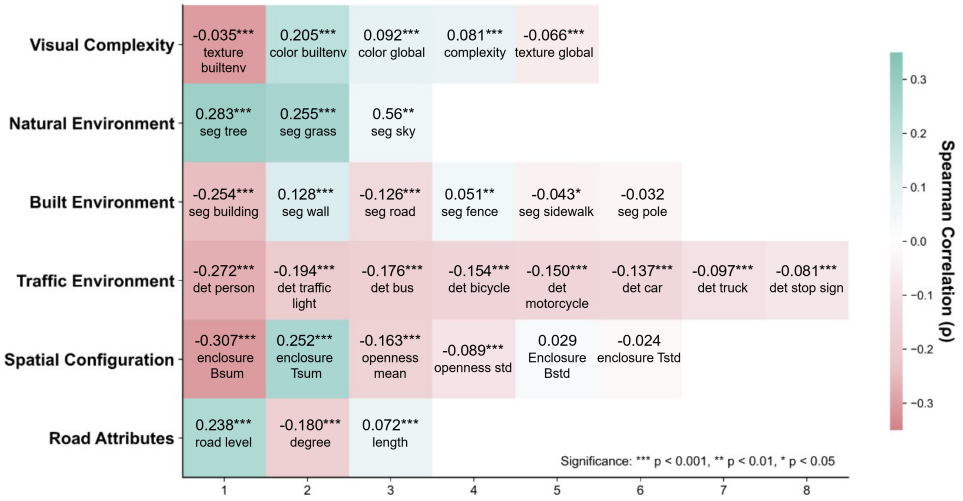

Figure 5: Correlation heatmap between environmental variables and perceived cycling safety. Rank denotes the ordering of variables based on the magnitude of their Pearson correlation.

4.2. Validation of RAGCN prediction model

To evaluate the performance of the proposed RAGCN model, we compared it with five baseline models: Logistic Regression, Random Forest, XGBoost, GCN, and GraphSAGE. All models were trained on the same feature set using an identical data partitioning strategy, with 70% of the data allocated for training, 10% for validation, and 20% for testing. Each experiment was repeated five times with

different random seeds, and results were averaged across all runs to ensure robustness in performance assessment.

Logistic Regression is a conventional statistical model for multi-class classification that assumes a linear relationship between predictors and the log-odds of the target classes, predicting class probabilities via the logistic function.

Random Forest (Breiman, 2001) is a tree-based ensemble model widely used in urban perception studies (Hamim and Ukkusuri, 2024), predicting class labels through majority voting across multiple decision trees. However, it treats samples independently and does not incorporate spatial or contextual dependencies.

XGBoost (Chen, 2016) is a gradient boosting framework that builds sequential decision trees to iteratively minimize residual errors, achieving strong predictive performance in various urban analytics tasks (Jin et al., 2025).

GCN (Kipf, 2016) is a seminal graph neural network model that integrates node attributes with graph topology through stacked convolutional layers, making it well-suited for spatially connected data such as road networks.

GraphSAGE (Hamilton et al., 2017) aggregates information from a node and its neighbors to generate node embeddings. Unlike GCN, which relies on a fixed adjacency matrix for full-neighborhood aggregation, it performs random neighbor sampling and applies learnable aggregation functions such as mean, LSTM, or pooling. In this study, the pooling aggregator is adopted. As an inductive framework, GraphSAGE can generalize to unseen nodes.

Note that Logistic Regression, Random Forest, and XGBoost only consider the feature vectors of the target road segment to classify its perceived cycling safety, while GCN, GraphSAGE, and our proposed RAGCN jointly consider its own features and those of its nearby segments.

As shown in Table 2, the proposed RAGCN model outperforms all five baselines, achieving the highest OA of 83.1% and a Macro F1 Score of 81.8%. Compared with Logistic Regression, Random Forest, and XGBoost, which rely solely on a road segment's own features and ignore its "geographic context", RAGCN improves accuracy by over 20%. Moreover, both Random Forest and XGBoost produce Kappa scores below 0.4, indicating limited ability to deliver consistent, non-random predictions of perceived cycling safety. Logistic Regression attains an accuracy of only 56.4%, falling short of RAGCN by 26.7%. The graph-based baselines, GCN and GraphSAGE, perform notably better than the non-graph models, underscoring the importance of incorporating the "geographic context" of a road segment. However, RAGCN still surpasses them across all metrics, with OA improvement 6.6%. These results demonstrate that RAGCN effectively captures both spatial dependencies and feature interactions, offering stable and accurate

predictions of perceived cycling safety in urban road networks.

Table 2: Classification performance of RAGCN and baseline models on perceived cycling safety.

Model	OA	Macro F1	Weighted F1	Kappa
LogisticRegression	56.4%	0.460	0.531	0.263
RandomForest	62.2%	0.549	0.601	0.364
XGBoost	61.4%	0.555	0.601	0.360
GraphSAGE	71.5%	0.695	0.718	0.552
GCN	76.5%	0.750	0.767	0.631
RAGCN (ours)	**83.1%**	**0.818**	**0.831**	**0.731**

In addition, we compared the performance of the adaptive loss with the standard CE loss (see Table 3). Under the same experimental settings, the model trained with CE loss achieved an OA of 82.8% and a Macro-F1 of 0.814, which are 0.3% and 0.4% lower, respectively, than those of our model. For the minority classes, the recalls of the safe and unsafe categories improved by 0.73% and 0.64%, respectively. These results indicate that the adaptive loss not only improves the overall accuracy but also contributes to balancing class-wise performance, particularly enhancing the recognition of minority classes.

Table 3: Comparison of model performance between CE loss and Adaptive loss.

Model	OA	Macro F1	Weighted F1	Kappa	Recall (Unsafe)	Recall (Safe)
CE loss	82.8%	0.814	0.828	0.725	77.7%	86.1%
Our loss	83.1%	0.818	0.831	0.731	78.4%	86.9%

4.3. Ablation studies

To evaluate the relative contribution of different feature dimensions to perceived cycling safety, we conducted ablation experiments by removing one of the six feature dimensions at a time and re-training the model to assess the independent effect of each dimension on predictive performance.

As presented in the left panel of Figure 6, excluding traffic environment features produced the largest performance decline, with OA dropping by 3.83%. This result underscores that traffic-related entities, such as cars and pedestrians, are critical determinants in shaping the safety perception of adolescents. Road Attributes and Visual Complexity emerged as similarly influential, suggesting that

both physical road design and visual diversity substantially affect cycling safety experiences. While road design is a well-established factor in cycling safety research (Lawson et al., 2013; Manton et al., 2016), our results highlight that visual cognition, driven by the complexity, also exerts a measurable influence. In addition, the removal of natural environment, spatial configuration, or built environment features each resulted in OA reductions exceeding 1.5%, indicating that these dimensions provide essential urban context for safety perception modeling. Collectively, these results confirm that perceived cycling safety emerges from the complex interplay of multidimensional environmental features.

Furthermore, to compare our multidimensional feature set with commonly used feature sets, two comparison scenarios are presented on the right panel of Figure 6. When only segmentation-based features (natural and built environmental elements) were used, the OA decreased by 3.0% compared with our full model, while the Weighted F1 and Macro F1 dropped by 2.9% and 3.3%, respectively. When both segmentation- and detection-based features (natural, built, and traffic environmental elements) were included, the OA was still 1.5% lower than that of our model, and the Weighted F1 and Macro F1 declined by 1.5% and 1.6%. These results collectively demonstrate the effectiveness of the proposed multidimensional feature framework in capturing diverse environmental determinants of perceived cycling safety.

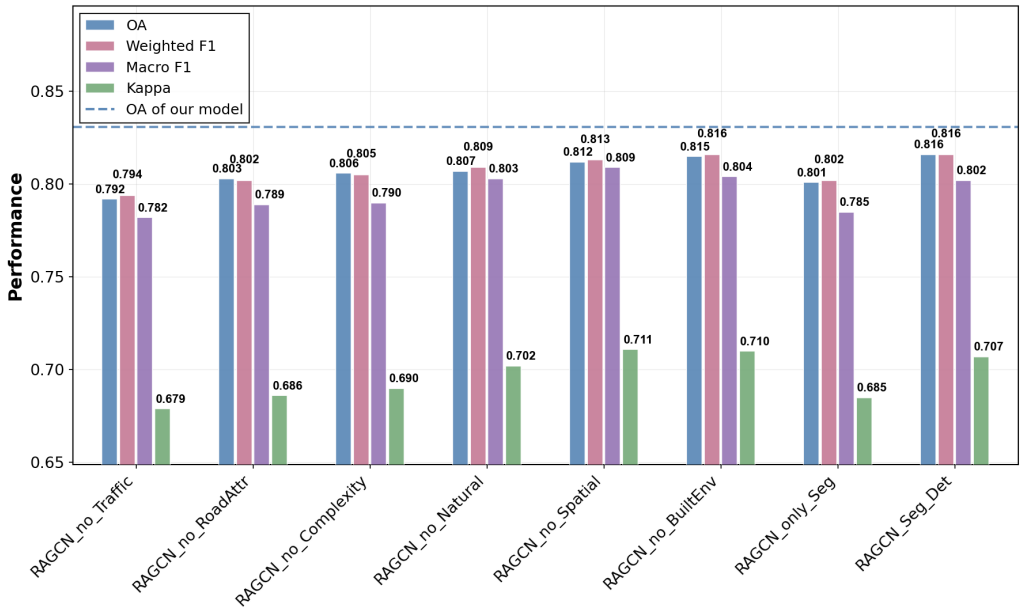

Figure 6: Ablation results of environmental dimensions.

4.4. Explaining the impact of features on perceived cycling safety

4.4.1. Global interpretation of feature contributions across perception categories

We applied GraphLIME to interpret the contribution of individual features on perceived cycling safety in the three categories of unsafe, neutral, and safe. Feature importance values represent the coefficients derived from the local subgraph of each target node. Figure 7 presents the feature importance scores from the RAGCN model and the relative contribution of each feature dimension across the three perception categories.

Among six feature groups, the traffic environment and the built environment play critical roles in shaping perceived cycling safety. It is notable that spatial configuration and visual complexity ranked second and third in contribution for the unsafe and safe perception categories, respectively. In detail, in segments perceived as unsafe, *det_person* and *seg_sidewalk* showed strong negative associations with perceived cycling safety. This suggests that unsafe cycling perception can be attributed to frequent cyclist–pedestrian interactions and the limited maneuvering space available for cyclists (Kang et al., 2013). In contrast, trees exhibited a mitigating effect on perceived unsafety, consistent with previous evidence highlighting greenery as a well-recognized environmental element promoting cycling (Brilhante and Klaas, 2018). Among spatial configuration indicators,

higher *openness_std*, which represents greater long-distance visibility, was associated with enhanced perceived safety. *texture_global* also contributed to alleviating perceived unsafety, indicating that richer visual textures, often corresponding to more diverse landscape textures (e.g., vegetation, tree canopies, and grassy areas), can balance the sense of environmental monotony and insecurity.

For safe segments, *det_motorcycle* was positively associated with higher perceived cycling safety. Although somewhat unexpected, this may be explained by local conditions where motorcycles and bicycles often share the same low-speed infrastructure (e.g., cycle streets and shared lanes). More motorcycles indicate a bicycle-friendly design rather than motorized dominance. Through manual inspection, minor misclassification of bicycles as motorcycles during detection could also contribute to this pattern. In contrast, the texture complexity of the built environment and both global and built-environment color complexity are identified as key negative contributors to perceived cycling safety. Streetscapes dominated by monotonous or excessively textured built environments tend to be associated with lower perceived cycling safety. On the one hand, overly intricate textures of the built environment can increase cognitive load (Guan et al., 2022), diverting cyclists' attention from traffic cues. On the other hand, uniform color schemes may reflect a lack of vitality in the streetscape, leading to negative emotional responses (Qi et al., 2025). Interestingly, *det_traffic light* showed contrasting effects across classes, positive for both unsafe and safe perceptions. This contradictory pattern is reasonable given the geographical heterogeneity of street environments. While traffic signals can regulate vehicle flow and maintain order, in areas with inadequate road infrastructure or high traffic density, they may instead result in potential hazards and conflicts (Strauss et al., 2014). For neutral segments, the main contributions were from dynamic traffic elements and traffic infrastructure. This finding underscores that the traffic environment is the dominant factor for the perception of cycling safety, acting as a mediator between perceived insecurity and safety.

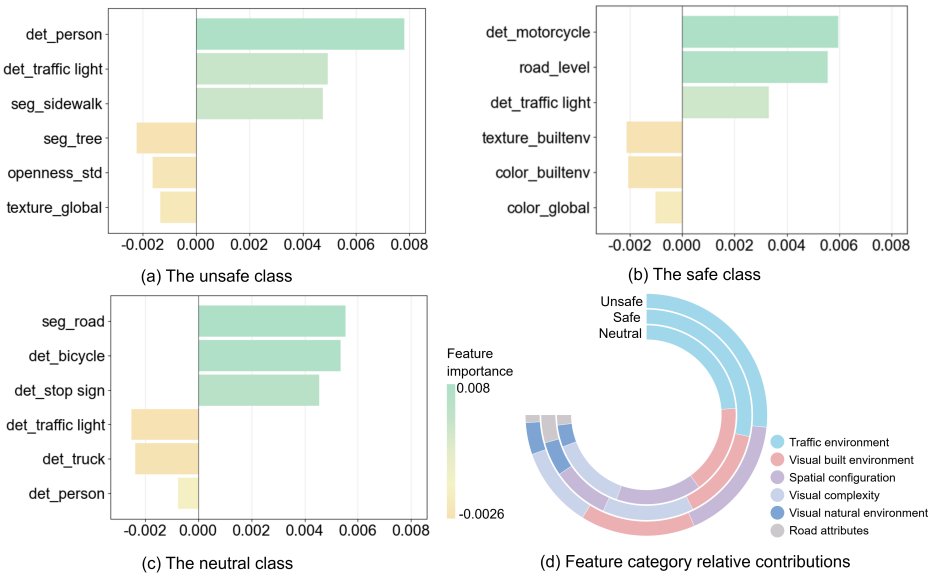

Figure 7: GraphLIME-based explanations of feature contributions to perceived cycling safety, based on RAGCN prediction results. The bar charts highlight the top three positive and negative features for each category. The positive coefficients indicate that increasing a feature raises the probability of the target class, while negative coefficients imply a decrease in that probability.

4.4.2. Local explanation of feature contributions: a case-based analysis

To further examine how urban environmental features jointly shape perceived cycling safety at the street level, we conducted a case-based analysis using representative segments (Figures 8 and 9). These examples illustrate how different environmental features influence perceived cycling safety within each segment. Segment 1092 is classified as unsafe, while Segment 6722 is classified as safe, allowing for a comparative interpretation across different urban conditions.

In Segment 1092, multiple dimensions jointly contribute to the prediction of low perceived cycling safety. A higher sky openness, represented by *seg_sky (40.945)*, reduces the likelihood of unsafe perception, suggesting that a more open sky view may alleviate spatial unsafe pressure. In terms of visual complexity, both global texture and color features show notable contributions. From a spatial configuration perspective, higher *openness_std*, reflecting better long-distance visibility, contributes positively to perceived safety. *det_traffic light* exhibits a negative contribution in this segment. Given that Segment 1092 is located on a major arterial road, traffic lights may be associated with higher traffic volumes and more complex interactions among road users. In this context, their presence may reflect

increased conflict potential.

In contrast, Segment 6722 demonstrates a different configuration of feature contributions associated with higher perceived cycling safety. In this segment, *det_traffic light* contributes positively. This segment is located on a tertiary road, where lower traffic intensity and simpler intersection structures may allow traffic lights to function more effectively as safety-supporting elements. At the same time, natural environment features such as *seg_tree* and *enclosure_Tstd* show negative contributions in Segment 6722. This indicates that trees located close to the roadway may obstruct visibility or create a sense of enclosure, potentially interfering with cyclists' perception of safety.

Overall, these case-based local explanations demonstrate that perceived cycling safety emerges from the combined effects of multiple feature dimensions, including traffic environment, built environment, natural environment, spatial configuration, and visual complexity. Rather than acting independently, these features interact within specific urban contexts to shape cyclists' perception.

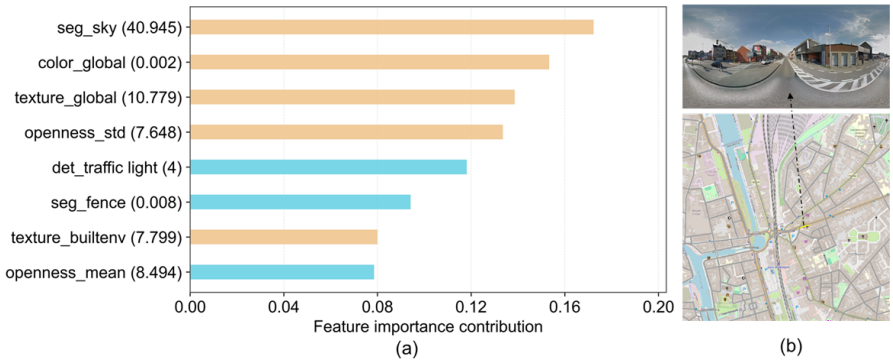

Figure 8: GraphLIME-based local explanation for Segment 1092. Blue indicates a positive contribution to the predicted class, while yellow indicates a negative contribution.

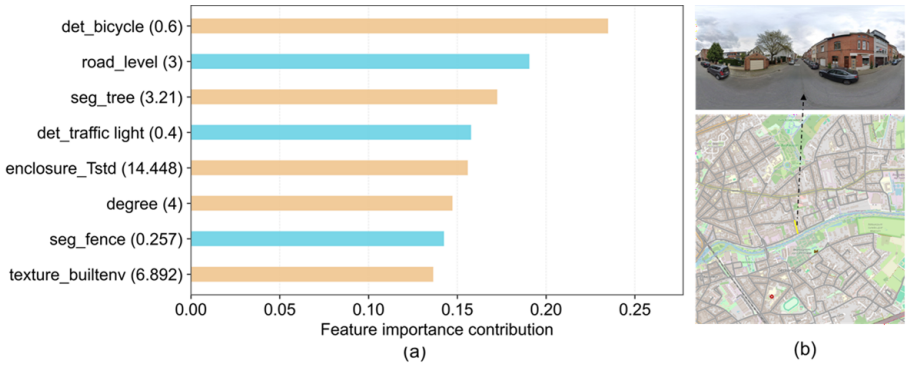

Figure 9: GraphLIME-based local explanation for Segment 6722. Blue indicates a positive contribution to the predicted class, while yellow indicates a negative contribution.

4.5. Mapping perceived cycling safety based on trained RAGCN

We examined the spatial distribution of perceived cycling safety by mapping the RAGCN predictions onto the entire road network, converting the softmax probability outputs into continuous safety scores. Consequently, the approach produced safety scores for 11,476 road segments in the study area. These scores were then analyzed using the Getis-Ord Gi* statistic to identify spatial clusters of high and low perceived safety. Figure 10 shows the predicted safety perception map, and Figure 11 presents the corresponding Gi* hotspot map.

Perceived cycling safety is lowest in the city center, with additional unsafe zones near the main train station, highway entrances, and university campuses. In contrast, living streets and internal residential roads form clear high-safety clusters, and northern neighborhoods tend to score higher on safety perception than southern ones. Some highway-adjacent segments are classified as neutral, likely due to parallel cycling lanes.

Figures 10 also present illustrative examples, where the environment patterns differ markedly across urban settings. SVI inspection aligns with the trends revealed in our earlier analyses. Unsafe areas often exhibit higher building density, greater enclosure by the built environment, more vehicles, fewer trees, and lower color diversity. In contrast, safer areas typically feature fewer vehicles, richer scene colors, reduced building coverage, and increased greenery. These differences emphasize the role of multi-dimensional visual indicators in shaping perceived cycling safety, providing evidence for safety-oriented urban design for sustainable mobility.

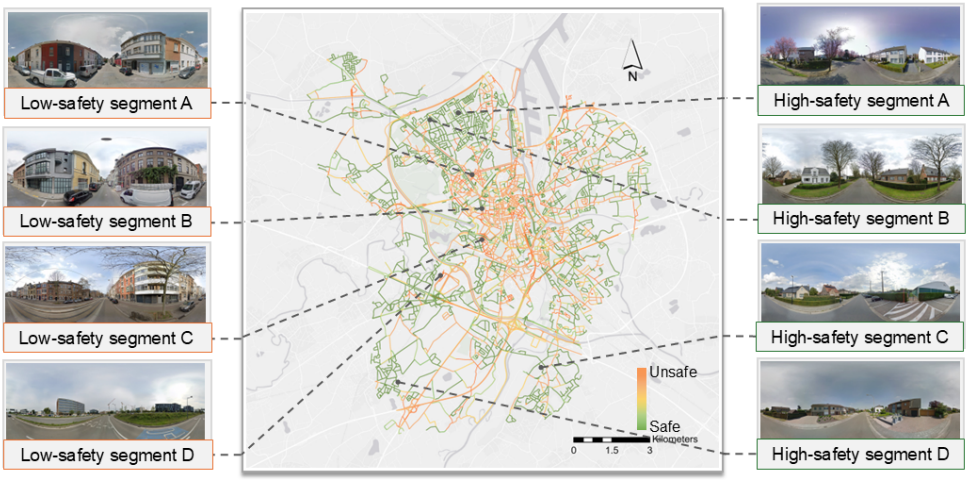

Figure 10: Predicted cycling safety perception across the road network, with an example road segment perceived as unsafe and safe.

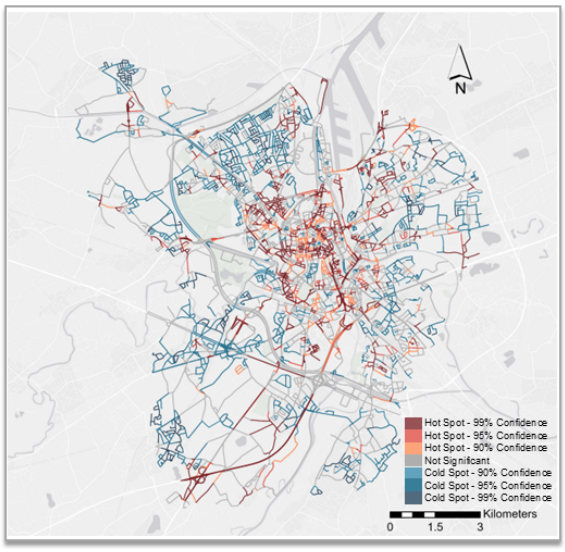

Figure 11: Gi* hotspot analysis showing statistically significant clusters of high and low perceived safety, with hot spots representing clusters of low safety perception (unsafe) and cold spots representing clusters of high safety perception (safe).

5. Discussion

5.1. Cycling Safety Perception Framework and AI-Driven Evidence

Perceived cycling safety reflects how individuals interact with the physical urban environment and is a key determinant influencing cycling uptake, route choice, and the willingness to engage in active travel. Most existing studies have examined isolated environmental attributes, often oversimplifying the interaction between human perception and urban context. To address this gap, we proposed a perception modeling framework that integrates SVI and road network data. This framework captures multidimensional visual and spatial features from the human perspective, encompassing six environmental dimensions: natural environment, built environment, traffic environment, spatial configuration, visual complexity, and road attributes, with 31 indicators, enabling a detailed and systematic assessment of street environment. Furthermore, this framework incorporates an enhanced GCN architecture (RAGCN) with explainable AI techniques to model the spatial dependencies among urban features and identify the key drivers of perceived cycling safety. Trained on labeled road segments, the framework produces interpretable outputs, allowing the identification of key environmental drivers of perceived cycling safety. This facilitates evidence-based prioritization of street improvements and micro-scale sustainable transport planning.

Based on our experiments and analyzes, the following major insights emerge. First, the proposed RAGCN, an extension of the GCN architecture enhanced with layer-wise attention and an adaptive loss function, achieves strong predictive performance, with an OA of 83.1% and a Cohen's Kappa of 0.731. It outperforms all baseline models, including GraphSAGE, GCN, random forest, XGBoost, and logistic regression. Relative to GraphSAGE and GCN, the RAGCN improves accuracy by 11.6% and 6.6%, respectively, underscoring its ability to model complex feature interactions in street-level contexts. The adaptive loss function further enhances the detection of unsafe segments, which are underrepresented in the data.

Second, our framework adopts a human-centered perspective by leveraging SVI to capture a diverse set of fine-grained features that mirror adolescents' on-road experiences. As a safety-sensitive cycling group, adolescents demonstrated heightened responsiveness to space-limiting and dynamic features in the XAI analysis: segments with high human activity and sidewalks were consistently associated with lower perceived safety, whereas trees and openness of road emerged as protective elements. Previous studies have similarly emphasized the role of greenery in enhancing perceived safety (Li et al., 2015), while pedestrian facilities have been strongly linked to perceptions of cyclists (Jensen, 2007). Ablation

experiments further verified the contribution of all feature dimensions. Compared with conventional SVI-based models that rely solely on segmentation-derived visual indicators, our multidimensional framework has improved OA and F1 scores by about 3%. This highlights the enhanced representational capacity of combining diverse visual and spatial features for modeling cycling safety perception. Among the six feature dimensions, traffic environment and built environment were underscored as dimensions of notable importance. High texture entropy in the built environment was associated with reduced perceived safety, aligning with evidence that irregular or heterogeneous visual environments heighten perceptual difficulty (Guan et al., 2022; Guo et al., 2018). In contrast, increased tree coverage and greater spatial depth of the road were associated with higher perceived cycling safety among adolescents, highlighting the role of natural elements and organized spatial structures in fostering safer traffic environments (Cai et al., 2022). Collectively, these findings illustrate the indispensable roles of visual environment and spatial cognition in shaping cycling safety, reinforcing the value of a perceptually aligned, multidimensional modeling approach.

Importantly, the proposed framework demonstrates strong potential for application across different urban contexts. As it relies on globally available SVI and road network data, it can be efficiently extended to other cities for large-scale evaluation. However, as cultural and spatial contexts may influence individual perceptions, the transferability of the model should be interpreted with caution. In particular, the current training data are not spatially uniform and may reflect context-specific travel patterns. Therefore, incorporating survey data from diverse cities and more spatially representative sampling strategies would be necessary to improve generalizability and reduce potential regional bias. Overall, the framework provides a flexible and interpretable tool for supporting active mobility planning, while highlighting the need for context-aware adaptation in broader applications.

5.2. Limitations and future work

Despite the demonstrated effectiveness of the proposed framework for predicting and explaining perceived cycling safety, several limitations should be acknowledged. First, the model validation employed a random split of road segments. In spatially dependent networks, this may lead to information leakage between training and testing sets if adjacent segments share similar visual features. Future work should implement spatial cross-validation (e.g., block-based splitting) to rigorously test generalizability to unseen neighborhoods.

Second, the current analysis relies primarily on environmental features extracted from SVI, which effectively capture the human-scale visual perspective but overlook other important dimensions of urban experience. A key missing dimension is the acoustic environment (i.e., urban soundscape), which has been shown to influence travel behavior and environmental perception (Gao and Fang, 2025a; Jeon and Jo, 2020). In addition, broader urban functional and socio-cultural dimensions remain underrepresented. Future studies should move toward a multisensory and multi-dimensional representation of cycling environments by integrating additional data sources, such as soundscape data (e.g., traffic noise levels or perceived acoustic environment), Points of Interest, socio-economic indicators, and human activity patterns. From the perspective of perception data, the current dataset is collected along school commuting routes, resulting in spatially uneven coverage that reflects real-world travel patterns. While frequently used corridors are represented, this also provides behaviorally grounded observations of cycling environments. Future work could further improve spatial representativeness by incorporating more diverse sampling strategies or additional datasets. Moreover, as participants focused on school-to-home routes, their prior knowledge, familiarity, and travel purposes may have introduced contextual biases in safety perception.

Third, the use of SVI introduces potential temporal bias. Although imagery was aligned closely with the perception survey period (around 2021), SVI may capture street environments under different temporal conditions. Seasonal variation, transient objects, and short-term activities can affect visual feature extraction. This limitation is particularly relevant during the COVID-19 period. As highlighted in recent studies (Wang et al., 2022; Ito et al., 2024), such temporal mismatches may introduce bias into the inferred effects of environmental factors. At the same time, leveraging multi-temporal SVI could facilitate the analysis of how perceived cycling safety responds to temporal changes in urban environments, supporting a more temporally explicit understanding of human–environment interactions.

Finally, while in our research we focused on a particular demographic group, for future work, it may be beneficial to understand variations of different subgroups on perception, e.g. taking into account gender and personality, as recent work has demonstrated their influence on the perception of visual urban environments (Quintana et al., 2025).

6. Conclusion

Perceived cycling safety is a key factor influencing travel choices and plays a crucial role in promoting a shift toward active mobility and shaping a human-centered urban environment focused on travel experience. This study investigates perceived cycling safety among adolescents to uncover how complex urban environments shape their safety perceptions. We first extracted diverse physical environment features from SVI and incorporated structural attributes of the road network. Building on this foundation, we developed an enhanced graph neural network model (RAGCN). Furthermore, XAI methods were employed to interpret how different environmental factors contribute to perceived cycling safety.

The proposed approach was evaluated using perceived cycling safety data collected in the city of Ghent. Results indicate that the RAGCN model outperforms all baseline models in both accuracy (83.1%) and Cohen's Kappa score (0.731), demonstrating its effectiveness in predicting perceived safety and its ability to differentiate among unsafe, neutral, and safe street segments. The ablation experiment further confirmed that the different feature dimensions contribute meaningfully to overall model performance. The XAI-based interpretation deepens our understanding of how specific features influence perceived safety: traffic-related elements, such as the number of visible persons and trucks, and visual complexity, such as the texture of the built environment, significantly affect perceived cycling safety. In terms of spatial configuration, greater variability in road openness tends to enhance perceived cycling safety, suggesting that streets with longer and more dynamic visibility ranges are perceived as safer.

This study presents a location-based perception modeling framework that enables learning and prediction at the road segment level. It aims to improve our understanding of how geographic entities (e.g., intersections and road segments) are perceived within urban spaces, and to provide practical support for fine-grained street design and sustainable urban development. Nonetheless, the current work primarily emphasizes model performance, with limited attention to model complexity and spatial generalization. Future research may extend this framework to different urban contexts and explore its applicability across different population groups, sample sizes, and urban contexts.

Declaration of Generative AI and AI-assisted technologies in the writing process

During the preparation of this work, the authors used ChatGPT for proofreading and improving the readability of the manuscript. After using this tool, the

authors reviewed and edited the content as needed and take full responsibility for the content of the publication.

Acknowledgments

We would like to express our sincere gratitude to Sien Benoit for her important contributions to the design and data collection of the Bike Barometer project. We would also like to thank Xiucheng Liang and Zicheng Fan for their helpful discussions and technical assistance during the early stages of this study.

This work was supported by the China Scholarship Council [grant number 202106270030] and Ghent University [grant number BOFCHN2021001101]. We gratefully acknowledge all data providers, including the Province of East Flanders, the City of Ghent, the OpenStreetMap community, and the contributors of Google Street View imagery. The Bike Barometer was developed with financial support from the Flemish Government. The first author would like to acknowledge the support of the European Institute of Innovation and Technology (EIT) Urban Mobility Doctoral Training Network.

Appendix A. Sensitivity Analysis of Label Discretization Schemes

To evaluate the robustness of the proposed classification scheme, we conducted a sensitivity analysis using three alternative discretization strategies for perceived cycling safety scores (0–10 scale): (1) the baseline scheme used in this study (0–4 = unsafe, 5 = neutral, 6–10 = safe), (2) an alternative threshold scheme (0–3 = unsafe, 4–6 = neutral, 7–10 = safe), and (3) a tertile-based binning approach based on percentile thresholds. All schemes were implemented within the same modeling framework (RAGCN), and their performance was evaluated using overall accuracy (OA), weighted F1, mean F1, and Cohen's Kappa.

Table A.1: Sensitivity analysis of different label discretization schemes for perceived cycling safety.

Scheme	OA	Macro F1	Weighted F1	Kappa	Class distribution
Baseline (0–4 / 5 / 6–10)	0.831	0.818	0.831	0.731	654 / 1049 / 1535
Alternative (0–3 / 4–6 / 7–10)	0.872	0.826	0.872	0.759	246 / 1918 / 1074
Tertile-based binning	0.850	0.816	0.850	0.750	1703 / 461 / 1074

The results show that all discretization schemes achieve consistently high predictive performance (OA $\geq$ 0.831), indicating that the proposed framework is robust to variations in label definitions. Although the alternative threshold scheme

yields slightly higher accuracy, it produces a highly imbalanced class distribution. In contrast, the baseline scheme produces a more balanced class distribution and is more consistent with the experimental design, which facilitates stable model training and interpretable results.

Overall, the consistency in model performance and interpretation across different schemes suggests that the findings of this study are not sensitive to the specific discretization strategy.

Appendix B. Rating Distribution and Perception Uncertainty

To examine variability in perceived cycling safety, we analyzed the distribution of the number of ratings per road segment and quantified within-segment disagreement using the interquartile range (IQR) (Figure B.1).

As shown in Figure B.1a, the number of ratings per segment is unevenly distributed, with a median of 4 and a mean of 7.54, indicating a long-tailed pattern. Figure B.1b shows that perceived safety is generally consistent across participants, with a median IQR of 1 and 25% of segments exhibiting no variability (IQR = 0). Most segments show low to moderate variability (IQR $\leq$ 2), while a small subset exhibits higher disagreement. As illustrated in Figure B.1c, perception variability is not solely driven by sample size, suggesting that disagreement may reflect intrinsic differences in how certain environments are perceived.

Overall, while median aggregation provides a stable representation for most segments, it may obscure variability in segments with high disagreement. Future work could incorporate uncertainty measures (e.g., IQR) into the modeling framework to better capture perception heterogeneity.

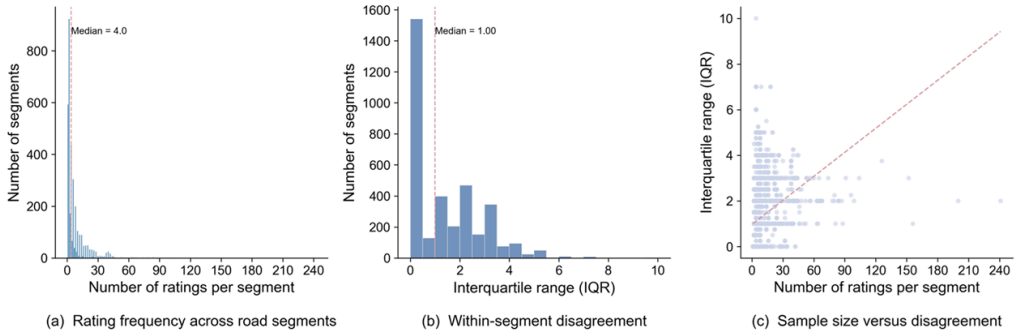

Figure B.1: Distribution of perception ratings and within-segment disagreement across road segments. (A) Distribution of the number of ratings per road segment. (B) Distribution of within-segment variability measured by the interquartile range (IQR). (C) Relationship between the number of ratings per segment and IQR.

References

Aldred, R., Goodman, A., Gulliver, J., Woodcock, J., 2018. Cycling injury risk in london: A case-control study exploring the impact of cycle volumes, motor vehicle volumes, and road characteristics including speed limits. Accident Analysis & Prevention 117, 75–84.

Arnold, H., 1993. Sustainable trees for sustainable cities. Arnoldia 53, 4–12.

Basaran, G.G., Kristoffersen, D., Haustein, S., 2021. Safety perceptions and cycling frequency of highly educated young people who grew up in different mobility cultures. Active Travel Studies 1.

Benoit, S., et al., 2022. Environmental factors associated with perceived cycling safety along adolescents' home-to-school routes. Journal of Location Based Services 16, 208–243.

Biljecki, F., Ito, K., 2021. Street view imagery in urban analytics and gis: A review. Landscape and Urban Planning 215, 104217.

Bill, E., Rowe, D., Ferguson, N., 2015. Does experience affect perceived risk of cycling hazards. STAR (Scottish Transport Applications Research) , 2015.

Black, P., Street, E., 2014. The power of perceptions: Exploring the role of urban design in cycling behaviours and healthy ageing. Transportation Research Procedia 4, 68–79.

Breiman, L., 2001. Random forests. Machine learning 45, 5–32.

Brilhante, O., Klaas, J., 2018. Green city concept and a method to measure green city performance over time applied to fifty cities globally: Influence of gdp, population size and energy efficiency. Sustainability 10, 2031.

Cai, Q., Abdel-Aty, M., Zheng, O., Wu, Y., 2022. Applying machine learning and google street view to explore effects of drivers' visual environment on traffic safety. Transportation research part C: emerging technologies 135, 103541.

Cao, Y., Yang, P., Xu, M., Li, M., Li, Y., Guo, R., 2025. A novel method of urban landscape perception based on biological vision process. Landscape and Urban Planning 254, 105246.

Chaurand, N., Delhomme, P., 2013. Cyclists and drivers in road interactions: A comparison of perceived crash risk. Accident Analysis & Prevention 50, 1176–1184.

Chen, D., Feng, Y., Li, X., Qu, M., Luo, P., Meng, L., 2025a. Interpreting core forms of urban morphology linked to urban functions with explainable graph neural network. arXiv preprint arXiv:2502.16210 .

Chen, N., Wang, L., Xu, T., Wang, M., 2025b. Perception of urban street visual color environment based on the cep-kass framework. Landscape and Urban Planning 259, 105359.

Chen, T., 2016. Xgboost: A scalable tree boosting system. Cornell University .

Cho, G., Rodríguez, D.A., Khattak, A.J., 2009. The role of the built environment in explaining relationships between perceived and actual pedestrian and bicyclist safety. Accident Analysis & Prevention 41, 692–702.

Cohen, J., 1960. A coefficient of agreement for nominal scales. Educational and psychological measurement 20, 37–46.

Costa, M., Wilhelm Siebert, F., Azevedo, C.L., Marques, M., Moura, F., 2024. Understanding perception of cycling safety from street-view images: uncovering non-linear effects of urban factors. This work has been submitted to the Elsevier for possible publication. Copyright may be transferred without notice, after which this version may no longer be accessible .

Cui, Q., Zhang, Y., Yang, G., Huang, Y., Chen, Y., 2023. Analysing gender differences in the perceived safety from street view imagery. International journal of applied earth observation and geoinformation 124, 103537.

Dacey, D.M., Liao, H.W., Peterson, B.B., Robinson, F.R., Smith, V.C., Pokorny, J., Yau, K.W., Gamlin, P.D., 2005. Melanopsin-expressing ganglion cells in primate retina signal colour and irradiance and project to the lgn. Nature 433, 749–754.

Elsheshtawy, Y., 1997. Urban complexity: toward the measurement of the physical complexity of street-scapes. Journal of Architectural and Planning Research , 301–316.

EU Urban Mobility Observatory, 2025. Ghent's approach to sustainable mobility planning: Aligning regional and city-level sumps.

European Commission, 2019. Road safety: European commission sets out next steps towards "vision zero", including key performance indicators.

Ewing, R., Handy, S., 2009. Measuring the unmeasurable: Urban design qualities related to walkability. Journal of Urban design 14, 65–84.

Fan, Z., Feng, C.C., Biljecki, F., 2025. Coverage and bias of street view imagery in mapping the urban environment. Computers, Environment and Urban Systems 117, 102253.

Álvaro Fernández-Heredia, Monzón, A., Jara-Díaz, S., 2014. Understanding cyclists' perceptions, keys for a successful bicycle promotion. Transportation Research Part A: Policy and Practice 63, 1–11.

Ferreira, M.C., Costa, P.D., Abrantes, D., Hora, J., Felício, S., Coimbra, M., Dias, T.G., 2022. Identifying the determinants and understanding their effect on the perception of safety, security, and comfort by pedestrians and cyclists: A systematic review. Transportation research part F: traffic psychology and behaviour 91, 136–163.

Friel, D., Wachholz, S., Werner, T., Zimmermann, L., Schwedes, O., Stark, R., 2023. Cyclists' perceived safety on intersections and roundabouts–a qualitative bicycle simulator study. Journal of safety research 87, 143–156.

Gao, M., Fang, C., 2025a. Decoding the impact of audiovisual street environment features on cycling volumes: Insights from street view imagery and machine learning. Transportation Research Part A: Policy and Practice 199, 104586.

Gao, M., Fang, C., 2025b. Pedaling through the cityscape: Unveiling the association of urban environment and cycling volume through street view imagery analysis. Cities 156, 105573.

Garcin, F., Xia, L., Faltings, B., 2013. How aggregators influence human rater behavior, in: Proc. Workshop@ 14th ACM Conference on Electronic Commerce (EC-13), pp. 1–12.

Garling, T., Book, A., Lindberg, E., 1984. Cognitive mapping of large-scale environments: The interrelationship of action plans, acquisition, and orientation. Environment and behavior 16, 3–34.

Geiger, A., Lenz, P., Urtasun, R., 2012. Are we ready for autonomous driving? the kitti vision benchmark suite, in: 2012 IEEE conference on computer vision and pattern recognition, IEEE. pp. 3354–3361.

Graystone, M., Mitra, R., Hess, P.M., 2022. Gendered perceptions of cycling safety and on-street bicycle infrastructure: bridging the gap. Transportation research part D: transport and environment 105, 103237.

Gu, Y., Quintana, M., Liang, X., Ito, K., Yap, W., Biljecki, F., 2025. Designing effective image-based surveys for urban visual perception. Landscape and Urban Planning 260, 105368.

Guan, F., Fang, Z., Wang, L., Zhang, X., Zhong, H., Huang, H., 2022. Modelling people's perceived scene complexity of real-world environments using street-view panoramas and open geodata. ISPRS Journal of Photogrammetry and Remote Sensing 186, 315–331.

Guo, Q., Hong, S., Tong, D., Xin, M., Gong, Y., Liu, Y., 2026. A partial prior knowledge framework to discover the cycling visual environment coupling street view images and shared bike trajectory using deep learning. Engineering Applications of Artificial Intelligence 165, 113457.

Guo, X., Qian, Y., Li, L., Asano, A., 2018. Assessment model for perceived visual complexity of painting images. Knowledge-Based Systems 159, 110–119.

Hamilton, W., Ying, Z., Leskovec, J., 2017. Inductive representation learning on large graphs. Advances in neural information processing systems 30.

Hamim, O.F., Ukkusuri, S.V., 2024. Towards safer streets: A framework for unveiling pedestrians' perceived road safety using street view imagery. Accident Analysis & Prevention 195, 107400.

Harvey, C., Aultman-Hall, L., Hurley, S.E., Troy, A., 2015. Effects of skeletal streetscape design on perceived safety. Landscape and Urban Planning 142, 18–28.

Harvey, J., Thorpe, N., Caygill, M., Namdeo, A., 2014. Public attitudes to and perceptions of high speed rail in the uk. Transport Policy 36, 70–78.

Haustein, S., Koglin, T., Nielsen, T.A.S., Svensson, Å., 2020. A comparison of cycling cultures in stockholm and copenhagen. International journal of sustainable transportation 14, 280–293.

Heath, T., Smith, S.G., Lim, B., 2000. Tall buildings and the urban skyline: The effect of visual complexity on preferences. Environment and behavior 32, 541–556.

Huang, Q., Yamada, M., Tian, Y., Singh, D., Chang, Y., 2022. Graphlime: Local interpretable model explanations for graph neural networks. IEEE Transactions on Knowledge and Data Engineering 35, 6968–6972.

Huber, S., Lindemann, P., Schröter, B., 2024. Safety and bicycle route choice: To what extent do accident risk and perceived safety influence bicycle route choice? Transportation Engineering 18, 100240.

Ito, K., Biljecki, F., 2021. Assessing bikeability with street view imagery and computer vision. Transportation research part C: emerging technologies 132, 103371.

Ito, K., Kang, Y., Zhang, Y., Zhang, F., Biljecki, F., 2024. Understanding urban perception with visual data: A systematic review. Cities 152, 105169. URL: https://www.sciencedirect.com/science/article/pii/S0264275124003834, doi:https://doi.org/10.1016/j.cities.2024.105169.

Janowicz, K., Gao, S., McKenzie, G., Hu, Y., Bhaduri, B., 2020. Geoai: spatially explicit artificial intelligence techniques for geographic knowledge discovery and beyond.

Janssens, D., Paul, R., Wets, G., 2020. Onderzoek verplaatsingsgedrag vlaanderen 5.5 (2019–2020) tabellenrapport. URL https://assets. vlaanderen. be/image/upload/v1606421215/OVG_5. 5_-_Tabellenrapport. pdf .

Jensen, S.U., 2007. Pedestrian and bicyclist level of service on roadway segments. Transportation research record 2031, 43–51.

Jeon, J.Y., Jo, H.I., 2020. Effects of audio-visual interactions on soundscape and landscape perception and their influence on satisfaction with the urban environment. Building and Environment 169, 106544.

Jin, T., Wei, X., Cheng, L., Wang, K., Xin, Y., Witlox, F., 2025. Street matters: Linking perceived street environment to older adults' bike-sharing. Travel Behaviour and Society 41, 101071.

Kang, L., Xiong, Y., Mannering, F.L., 2013. Statistical analysis of pedestrian perceptions of sidewalk level of service in the presence of bicycles. Transportation Research Part A: Policy and Practice 53, 10–21.

Kang, Y., Abraham, J., Ceccato, V., Duarte, F., Gao, S., Ljungqvist, L., Zhang, F., Näsman, P., Ratti, C., 2023. Assessing differences in safety perceptions using geoai and survey across neighbourhoods in stockholm, sweden. Landscape and Urban Planning 236, 104768.

Kawshalya, L., Weerasinghe, U., Chandrasekara, D., 2022. The impact of visual complexity on perceived safety and comfort of the users: A study on urban streetscape of sri lanka. Plos one 17, e0272074.

Kim, G., Kim, A., Kim, Y., 2019. A new 3d space syntax metric based on 3d isovist capture in urban space using remote sensing technology. Computers, Environment and Urban Systems 74, 74–87.

Kim, Y.O., 1999. Spatial Configuration, Spatial Cognition and Spatial Behaviour: the role of architectural intelligibility in shaping spatial experience.

Kipf, T., 2016. Semi-supervised classification with graph convolutional networks. arXiv preprint arXiv:1609.02907 .

Klos, L., Eberhardt, T., Nigg, C., Niessner, C., Wäsche, H., Woll, A., 2023. Perceived physical environment and active transport in adolescents: a systematic review. Journal of Transport & Health 33, 101689.

Kummeneje, A.M., Rundmo, T., 2020. Attitudes, risk perception and risk-taking behaviour among regular cyclists in norway. Transportation research part F: traffic psychology and behaviour 69, 135–150.

Kwan, M.P., 2007. Mobile communications, social networks, and urban travel: Hypertext as a new metaphor for conceptualizing spatial interaction. The Professional Geographer 59, 434–446.

Lakshminarayanan, B., Teh, Y.W., 2013. Inferring ground truth from multi-annotator ordinal data: a probabilistic approach. arXiv preprint arXiv:1305.0015 .

Lawson, A.R., Pakrashi, V., Ghosh, B., Szeto, W., 2013. Perception of safety of cyclists in dublin city. Accident Analysis & Prevention 50, 499–511.

Lei, B., Liu, P., Liang, X., Yan, Y., Biljecki, F., 2025. Developing the urban comfort index: Advancing liveability analytics with a multidimensional approach and explainable artificial intelligence. Sustainable Cities and Society 120, 106121.

Li, X., Zhang, C., Li, W., 2015. Does the visibility of greenery increase perceived safety in urban areas? evidence from the place pulse 1.0 dataset. ISPRS International Journal of Geo-Information 4, 1166–1183.

Liu, P., Zhang, Y., Biljecki, F., 2024. Explainable spatially explicit geospatial artificial intelligence in urban analytics. Environment and Planning B: Urban Analytics and City Science 51, 1104–1123.

Liu, P., Zhao, T., Luo, J., Lei, B., Frei, M., Miller, C., Biljecki, F., 2023. Towards human-centric digital twins: Leveraging computer vision and graph models to predict outdoor comfort. Sustainable Cities and Society 93, 104480.

Lonergan, C., Hedley, N., 2016. Unpacking isovists: a framework for 3d spatial visibility analysis. Cartography and Geographic Information Science 43, 87–102.

Manton, R., Rau, H., Fahy, F., Sheahan, J., Clifford, E., 2016. Using mental mapping to unpack perceived cycling risk. Accident Analysis & Prevention 88, 138–149.

Martínez-Díaz, M., Arroyo, R., 2023. Is cycling safe? does it look like it? insights from helsinki and barcelona. Sustainability 15, 905.

Mertens, L., Van Cauwenberg, J., Ghekiere, A., Van Holle, V., De Bourdeaudhuij, I., Deforche, B., Nasar, J., Van de Weghe, N., Van Dyck, D., 2015. Does the effect of micro-environmental factors on a street's appeal for adults' bicycle transport vary across different macro-environments? an experimental study. PloS one 10, e0136715.

Nippani, A., Li, D., Ju, H., Koutsopoulos, H., Zhang, H., 2023. Graph neural networks for road safety modeling: Datasets and evaluations for accident analysis. Advances in neural information processing systems 36, 52009–52032.

Olsson, S.R., Elldér, E., 2023. Are bicycle streets cyclist-friendly? micro-environmental factors for improving perceived safety when cycling in mixed traffic. Accident analysis & prevention 184, 107007.

Porteous, J.D., 2013. Environmental aesthetics: Ideas, politics and planning.

Purciel, M., Neckerman, K.M., Lovasi, G.S., Quinn, J.W., Weiss, C., Bader, M.D., Ewing, R., Rundle, A., 2009. Creating and validating gis measures of urban design for health research. Journal of environmental psychology 29, 457–466.

Qi, Z., Li, J., Yang, X., He, Z., 2025. How the characteristics of street color affect visitor emotional experience. Computational Urban Science 5, 7.

Quintana, M., Gu, Y., Liang, X., Hou, Y., Ito, K., Zhu, Y., Abdelrahman, M., Biljecki, F., 2025. Global urban visual perception varies across demographics and personalities. Nature Cities 2, 1092–1106. doi:10.1038/s44284-025-00330-x.

Rahman, M.L., Moore, A.B., Mandic, S., 2022. Adolescents' perceptions of school neighbourhood built environment for walking and cycling to school. Transportation research part F: traffic psychology and behaviour 88, 111–121.

Ren, S., He, K., Girshick, R., Sun, J., 2016. Faster r-cnn: Towards real-time object detection with region proposal networks. IEEE transactions on pattern analysis and machine intelligence 39, 1137–1149.

Rietveld, R., Van Dolen, W., Mazloom, M., Worring, M., 2020. What you feel, is what you like influence of message appeals on customer engagement on instagram. Journal of interactive marketing 49, 20–53.

van Rijswijk, L., Rooks, G., Haans, A., 2016. Safety in the eye of the beholder: Individual susceptibility to safety-related characteristics of nocturnal urban scenes. Journal of Environmental Psychology 45, 103–115.

Rui, J., Xu, Y., 2024. Beyond built environment: Unveiling the interplay of streetscape perceptions and cycling behavior. Sustainable Cities and Society 109, 105525.

Sanocki, T., Islam, M., Doyon, J.K., Lee, C., 2015. Rapid scene perception with tragic consequences: observers miss perceiving vulnerable road users, especially in crowded traffic scenes. Attention, Perception, & Psychophysics 77, 1252–1262.

Schepers, P., Hagenzieker, M., Methorst, R., van Wee, B., Wegman, F., 2014. A conceptual framework for road safety and mobility applied to cycling safety. Accident analysis & prevention 62, 331–340.

Schönbach, D., Altenburg, T., Marques, A., Chinapaw, M., 2020. Strategies and effects of school-based interventions to promote active school transportation by bicycle among children and adolescents: a systematic review. International Journal of Behavioral Nutrition and Physical Activity 17, 138.

Sokolova, M., Lapalme, G., 2009. A systematic analysis of performance measures for classification tasks. Information processing & management 45, 427–437.

Stamps III, A.E., 2005. Enclosure and safety in urbanscapes. Environment and behavior 37, 102–133.

Storme, T., Benoit, S., Van de Weghe, N., Mertens, L., Van Dyck, D., Brondeel, R., Witlox, F., Zwartjes, L., Cardon, G., 2022. Citizen science and the potential for mobility policy–introducing the bike barometer. Case Studies on Transport Policy 10, 1539–1549.

Strauss, J., Miranda-Moreno, L.F., Morency, P., 2014. Multimodal injury risk analysis of road users at signalized and non-signalized intersections. Accident Analysis & Prevention 71, 201–209.

Tapiro, H., Oron-Gilad, T., Parmet, Y., 2020. Pedestrian distraction: The effects of road environment complexity and age on pedestrian's visual attention and crossing behavior. Journal of safety research 72, 101–109.

Vandenbulcke, G., Thomas, I., Panis, L.I., 2014. Predicting cycling accident risk in brussels: A spatial case–control approach. Accident Analysis & Prevention 62, 341–357.

Vias institute, 2023. Elke dag raken 14 kinderen gewond in een verkeersongeval op weg naar of van school.

Wang, L., Han, X., He, J., Jung, T., 2022. Measuring residents' perceptions of city streets to inform better street planning through deep learning and space syntax. ISPRS Journal of Photogrammetry and Remote Sensing 190, 215–230.

Wang, L., Zhang, T., He, J., Kada, M., 2025. Cross-platform complementarity: Assessing the data quality and availability of google street view and baidu street view. Transactions in Urban Data, Science, and Technology 4, 22–47.

Wang, M., Zheng, D., Ye, Z., Gan, Q., Li, M., Song, X., Zhou, J., Ma, C., Yu, L., Gai, Y., et al., 2019. Deep graph library: A graph-centric, highly-performant package for graph neural networks. arXiv preprint arXiv:1909.01315 .

Wei, X., Li, J., Zhang, X., Gu, H., Van de Weghe, N., Huang, H., 2025. An innovative framework combining a cnn-transformer multiscale fusion network and spatial analysis for cycleway extraction using street view images. Sustainable Cities and Society , 106384.

Winters, M., Babul, S., Becker, H., Brubacher, J.R., Chipman, M., Cripton, P., Cusimano, M.D., Friedman, S.M., Harris, M.A., Hunte, G., et al., 2012. Safe cycling: how do risk perceptions compare with observed risk? Canadian journal of public health 103, S42–S47.

Wu, J., Hong, L., Frias-Martinez, V., 2018. Predicting perceived cycling safety levels using open and crowdsourced data, in: 2018 IEEE International Conference on Big Data (Big Data), IEEE. pp. 1669–1676.

Xie, E., Wang, W., Yu, Z., Anandkumar, A., Alvarez, J.M., Luo, P., 2021. Segformer: Simple and efficient design for semantic segmentation with transformers. Advances in neural information processing systems 34, 12077–12090.

Yap, W., Stouffs, R., Biljecki, F., 2023. Urbanity: automated modelling and analysis of multidimensional networks in cities. npj Urban Sustainability 3, 45.

Ye, Y., Zhong, C., Suel, E., 2024. Unpacking the perceived cycling safety of road environment using street view imagery and cycle accident data. Accident Analysis & Prevention 205, 107677.

Yin, W., Zhang, C., Chen, H., Cai, Z., Yu, G., Wang, K., Chen, X., Shen, C., 2023. Metric3d: Towards zero-shot metric 3d prediction from a single image, in: Proceedings of the IEEE/CVF international conference on computer vision, pp. 9043–9053.

Yu, B., Lee, Y., Sohn, K., 2020. Forecasting road traffic speeds by considering area-wide spatio-temporal dependencies based on a graph convolutional neural network (gcn). Transportation research part C: emerging technologies 114, 189–204.

Yue, H., 2025. Investigating streetscape environmental characteristics associated with road traffic crashes using street view imagery and computer vision. Accident Analysis & Prevention 210, 107851.

Zeng, Q., Gong, Z., Wu, S., Zhuang, C., Li, S., 2024. Measuring cyclists' subjective perceptions of the street riding environment using k-means smote-rf model and street view imagery. International Journal of Applied Earth Observation and Geoinformation 128, 103739.

Zhang, F., Wu, L., Zhu, D., Liu, Y., 2019. Social sensing from street-level imagery: A case study in learning spatio-temporal urban mobility patterns. ISPRS Journal of Photogrammetry and Remote Sensing 153, 48–58.

Zhang, M., Meng, L., 2007. An iterative road-matching approach for the integration of postal data. Computers, Environment and Urban Systems 31, 597–615.

Zhou, H., Gu, J., Liu, Y., Wang, X., 2022. The impact of the "skeleton" and "skin" for the streetscape on the walking behavior in 3d vertical cities. Landscape and Urban Planning 227, 104543.